Polymer Bulletin 53, 315–321 (2005)
DOI 10.1007/s00289-005-0342-0

Polymer Bulletin

Fabrication of Microporous Films Utilizing Amphiphilic Block Copolymers and Their Use as Templates in Poly(aniline) Preparation

Yuko Maeda, Yasuko Shimoi, Kenji Ogino (✉)

Graduate School of Bio-Applications and Systems Engineering, Tokyo University of Agriculture and Technology, Koganei, Tokyo 184-8588, Japan
E-mail: kogino@cc.tuat.ac.jp, Fax: +81-42-388-7404

Received: 10 November 2004 / Revised version: 24 January 2005 / Accepted: 25 January 2005

Summary

Ordered microporous films were fabricated on the process of solvent evaporation for the solution of amphiphilic poly(acrylic acid)-*block*-polystyrene under a humid atmosphere. Pore size and its distribution are strongly dependent on the nature of polymers and the evaporation conditions. Poly(aniline) dots were also successfully fabricated via electropolymerization of aniline using a microporous film on indium tin oxide electrode as a template.

Introduction

Recently a simple non-template method by self-assembly of block copolymers [1-6] and amphiphiles [7, 8] have been used for the fabrication of highly ordered microporous polymer films with honeycomb structure. The route to the formation of a regular pattern can be provided by dissipative processes, where controlled condensation and growth of water droplets on the cold surfaces resulting from solvent evaporation of polymer solutions may be used to create a patterned surface. Srinivasarao et al. fabricated 2D or 3D porous layered films utilizing polystyrene with carboxyl end group by controlling solvent density [9] and more recently Peng et al. reported that appropriate choice of solvents, and molecular weight, polystyrenes without polar groups afforded ordered patterns [10]. The utilization of block copolymer gives rise to another advantage because of microphase separation or surface aggregation. Hayakawa et al. reported that using a specially designed block copolymer, resulting porous films have highly ordered hierarchical structures over multiple length scales from angstroms to micrometers [6].

In this report, poly(acrylic acid)-*block*-poly(styrene) was chosen to fabricate the microporous films. Hydrophilic poly(acrylic acid) block impedes the coalescent of water droplets by efficient adsorption at the water/polymer interface and stabilized the regularity resulting in the ordered pattern after the solvent evaporation. It is strongly expected that the microphase separated hydrophilic block dominates the pore surfaces and is subject to further chemical modification. The relationships between the conditions in the film fabrication and pore size and its distribution were investigated utilizing block copolymers with different block length. As a preliminary application of porous films, poly(aniline) dots were fabricated via electrochemical polymerization using a porous film on indium tin oxide electrode as a template.

Experimental

Synthesis of macroinitiators

The preparation of macroinitiator was carried out by procedures similar to that published in the literature [11-13]. A 100-ml three necked flask equipped with a stirrer bar, a nitrogen inlet, and a rubber septum was charged with CuBr (0.74 g, 5.2 mmol), $CuBr_2$ (0.058 g, 0.26 mmol) under nitrogen. After the evacuation followed with backfilling of nitrogen, distilled *tert*-butyl acrylate (tBA, 40 g, 0.31 mol) was added via gas-tight syringe followed by N,N,N',N",N"- pentamethyldiethylenetriamine (PMDETA, 2.17 ml, 10.4 mmol) and acetone (5 ml). After two freeze-pump-thaw cycles, *tert*-butyl 2-bromopropionate (1.72 ml, 10.4 mmol) was added and the mixture was allowed to stir at room temperature for 10 min. The flask was then placed in a 60°C oil bath and the polymerization proceeded for 4 h under nitrogen atmosphere. After 2 h, 5-ml of reaction mixture was removed via gas-tight syringe. THF solutions of reaction mixtures were filtered with an Al_2O_3/SiO_2 plug in order to remove the catalysts. After the concentration of solution, the polymers were precipitated into 50 vol% of methanol/H_2O mixture. The degree of polymerization was determined by the end group analysis based on ^{1}H-NMR spectroscopy. The polymerization of styrene (St, 20 ml, 174 mmol) was also conducted at 80°C for 12 h using methyl 2-bromopropionate (97 μl, 0.87 mmol), PMDETA (183 μl, 0.87 mmol), CuBr (125 mg, 0.87 mmol) and anisole (4 ml).

Synthesis of block copolymers

Using P(tBA) or PSt macroinitiator, block copolymers were synthesized. In the case of P(tBA), styrene (100 equivalent to the macroinitiator) was polymerized at 90°C for 12-24 h using PMDETA and CuBr (both equivalent to the macroinitiator). Purification procedures were similar to that mentioned above. tBA (20 equivalent to the P(St) macroinitiator) was polymerized using anisole as a solvent (twofold amount of tBA). The resulting block copolymer was dissolved in an equal weight of dioxane with a catalytic amount of *p*-toluene sulfonic acid monohydrate. The reaction mixture was refluxed for 10 h to eliminate *tert*-butyl group.

Fabrication of microporous films

Carbon disulfide solution (0.05-0.1 wt%, 50 μl) was drop-cast on a cleaned glass slide or an indium tin oxide (ITO) covered glass over an area of ca. 1.1 cm^2 (circle with a diameter of 1.2 cm) in a custom designed flow-hood (640 cm^3). The humidity was kept at 75 or 100% at 25°C by bubbling the air through a reservoir containing saturated NaCl solution or water, respectively. The flow-rates were controlled to be 5-20 L/min using a flow meter.

Electrochemical polymerization of aniline

Electropolymerization of aniline on the ITO-coated glass with or without a porous film was carried out using a three-electrode setup. A platinum spiral served as a counter electrode and Ag/AgCl as a reference electrode. Aqueous electrolyte consisted of 2.0 M perchloric acid and 0.5 M aniline. The polymerization was carried out by cycling the potential from 0 to 1.5 V for 6 cycles at a 300 mV/s rate using Nikko Keisoku potentiogalvanostat (NPGFZ-2501-A). A template was removed by immersing the substrate in THF.

Measurements

NMR spectra were recorded at 50°C with a JEOL α-500 spectrometer operating at 500 MHz for ^{1}H. The molecular masses of synthesized polymers were estimated by gel permeation chromatography using a column packed with styrene-divinylbenzene gel beads [14]. THF was used as an eluent and the molecular mass was calibrated using poly(styrene) standards (Shodex). Optical microscope (Keyence, VH-8000) images were used to determine the average open pore diameter and its distribution of fabricated films by counting the diameters for 100 pores. Morphology of poly(aniline) films were observed using scanning electron microscope (Hitachi S-4500).

Results and Discussion

Synthesis of amphiphilic block copolymers

Atom transfer radical polymerization of acrylic acid (AA) is shown to be unsuccessful because of the side reaction between monomer and Cu(II) deactivator [15]. Therefore P(AA) blocks were built by the hydrolysis of tBA moiety. The utilization of *tert*-butyl 2-bromopropionate as an initiator made it possible to exclude the end group effect on the formation of pores. ^{1}H-NMR signals for the end groups (C**H**$_3$CH, and C**H**Br) for P(tBA) resonated at 1.1 and 4.1 ppm in CDCl$_3$, respectively, and the degree of polymerization (DP) was determined based on the relative intensities of these signals to others. As expected, DP could be controlled by varying the polymerization time. Block length for P(St) was calculated from the chemical composition of the copolymer. In order to obtain the block copolymers with the same P(St) block length, P(St) macroinitiator was also utilized. Elimination of *tert*-butyl group was confirmed by the disappearance of *tert*-butyl resonance at 1.4 ppm in ^{1}H-NMR spectrum, and the doublet absorption observed in 1350-1400 cm^{-1} (CH$_3$ deformation) in IR spectrum. Table 1 lists the characteristics of block copolymers used in this study.

Table 1. Characteristics of amphiphilic block copolymers

Copolymer	St block	AA block	$M_n{}^a/10^4$	$M_w/M_n{}^a$
1	73	10	1.3 (0.9)	1.2
2	89	14	1.4 (1.1)	1.3
3	97	5	1.2 (1.0)	1.4
4	97	9	1.3 (1.1)	1.4

Copolymers 1,2; prepared with P(tBA) macroinitiators with different length, Copolymers 3, 4; prepared with the same P(St) macroinitiotor, a): determined by GPC for the samples before the elimination of *tert*-butyl group (THF eluent, P(St) standards). The values in parentheses designate the values based on ^{1}H-NMR analyses.

Fabrication of porous films

After placing 50 µl of CS_2 solution over an area of ca. 1.1 cm^2 on a glass slide in flow-food (air flow across the surface), the solvent began to evaporated, and the transparent solution became turbid due to the appearance of condensed water droplets. After the complete evaporation of solvent, an semitransparent film left behind. Due to the faster evaporation at the edge of solution, the film thickness and the resulting pore size were smaller in the peripheral region than the central area. The central circle with the diameter with 0.6 mm seemed homogeneous from the view point of the film thickness and the pore size. The following results about pore size and its distribution are for the central area. Figure 1 shows that highly ordered porous films with open pore size of 5.4 µm were obtained. Light scattering pattern (Fig.1b) indicates the perfect hexagonal arrangements of pores.

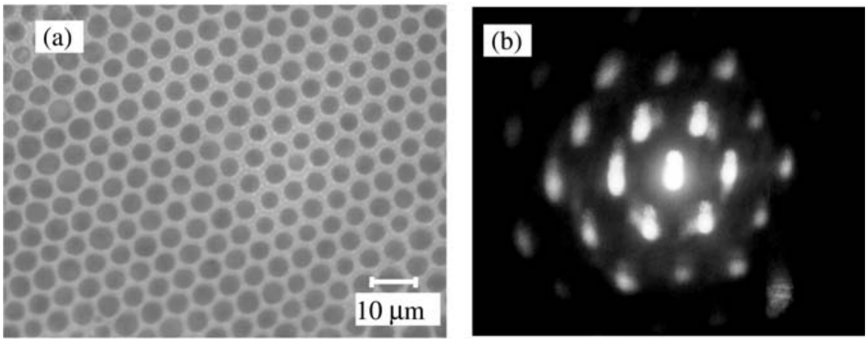

Figure 1. Microporous film fabricated using polymer 1 (concentration 0.1 wt%, flow rate 20 L/min, humidity 100 %), a): optical micrograph, b) light scattering image with He-Ne laser

The resulting pore size and its distribution were strongly dependent on the characteristics of polymers and the fabrication conditions. In Figure 2a the pore size and the coefficient of variation (CV) are plotted against the flow rate for the different concentration samples (copolymer 1). With the increase of the flow rate, the resulting pore size increased, while the CV values decreased. Lower initial polymer concentration afforded the larger pore size. In the initial stage of solvent evaporation, it is speculated that the number of nuclei formed increases with the increase of polymer concentration and the amount of condensed water is almost the same each other, leading to the smaller pores. Steyer et al. [16] have suggested that the growth of breath figures on liquids evolves through three stages. At the initial stage, the surface coverage by water droplets is low and each droplet grows with small interdroplets interaction. The mobility of the droplet is higher than that in the following stages. At the low flow rate, the initial stage prolongs, which leads to higher probability of coalescent of droplets, resulting in relatively disordered films. As Peng et al. reported [10], the lower humidity (75%) decreased the pore size because of the decrease of the amount of condensed water.

In Figure 2b, the flow rate dependence of resulting pores was indicated for the different polymers. As discussed above, the higher was the flow rate, the larger was the pore for all copolymers examined. It is found that the pore size for copolymer 4 was smaller than for copolymers 1 and 3 especially at the higher flow rate region. Copolymer 4 has almost the same length of AA block and the longer St block

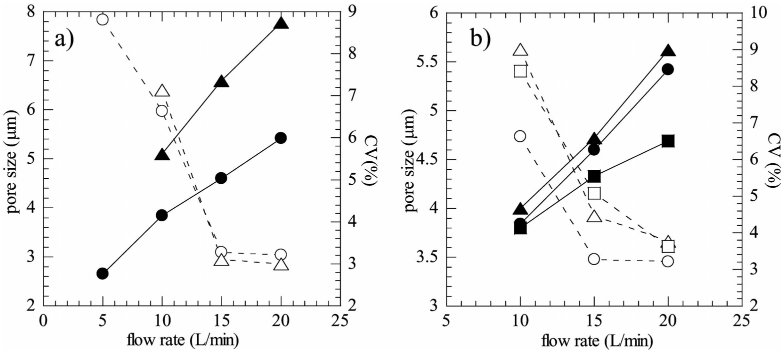

Figure 2. Flow rate dependence of the pore size and its distribution. Filled and open symbols represent pore size and CV value, respectively. (a): Initial concentration of polymer was 0.05 (triangle) and 0.1 wt% (circle), respectively for copolymer 1, (b) circle: copolymer 1, triangle; copolymer 3, square; copolymer 4, concentration; 0.1 wt%

compared with copolymer 1, and has the same St block and the shorter AA block compared with copolymer 3. The number of nuclei in the initial stage probably increased with the increase of hydrophilic AA block length, resulting in the smaller pore size. The reason why copolymer 4 afforded smaller pores than copolymer 1 although the hydrophilic length is almost the same each other is as follows. When the solvent evaporates, the concentration of polymer increases leading to the increase of viscosity at the air-solution interface. It is considered that the longer is the styrene block length, the more the viscosity increases. As a result, the solvent evaporation is more suppressed for copolymer 4 due to the formation of the hard shell layer on the top of the solution. The lower evaporation rate resulted in the smaller pores for copolymer 4. Only disordered films were obtained for copolymer 2 (hydrophilic AA block length: 14) on the experimental conditions we examined here. Too much hydrophilic nature allowed the formation of new nuclei after the initial stage of the solvent evaporation, resulting in the polydispersed pores.

Poly(aniline) synthesis

The pore size of the films fabricated on ITO covered glass was slightly larger than on the normal glass slides. Hydrophobic nature or surface roughness may influence the final pore size. For the electrochemical polymerization of aniline, the microporous film with 4.6 μm pore diameter was fabricated using copolymer 1 at the flow rate of 15 L/min, and the relative humidity of 75%. Figure 3 represents scanning electron micrographs of poly(aniline)s prepared with (a and b) and without (c and d) the polymer template. The template was washed out by immersing the substrate in THF. As shown in Fig. 3a, the open pores were successfully filled with deposited poly(aniline), and the diameter of poly(aniline) disk was comparable to that of the pore of the template. Inverse opals of poly(aniline) or other conducting polymers were fabricated by chemical or electrochemical polymerization using the colloidal crystal templates [17-19]. Guan et al. [20] recently reported the fabrication of patterned poly(aniline) microstructure using a template fabricated with a microcontact printing method. In these reports, the ordered porous structures form in the micrometer range, however little attention has been paid to the structural morphology of formed poly(aniline) on the nanometer scale.

It is noteworthy that the dense and smooth morphology was obtained with the template polymer, while the polymer has an open structure with entangled fibrous morphology without a template (Figs. 3 a and c). This observation was also confirmed at the higher magnification (Figs. 3 b and d). With the template, a very fine granular structure was interconnected each other and the diameter of each particle was less than 40 nm. On the other hand, fiber bundles were formed with the relatively large voids. The growth of poly(aniline) was much influenced by the presence of the template. The morphology of poly(aniline) prepared electrochemically is well-known to be changed by the experimental conditions including the growth methods, the type of electrolytes, and the concentration of reactants [21, 22]. Further investigation is necessary to control the morphology as desired.

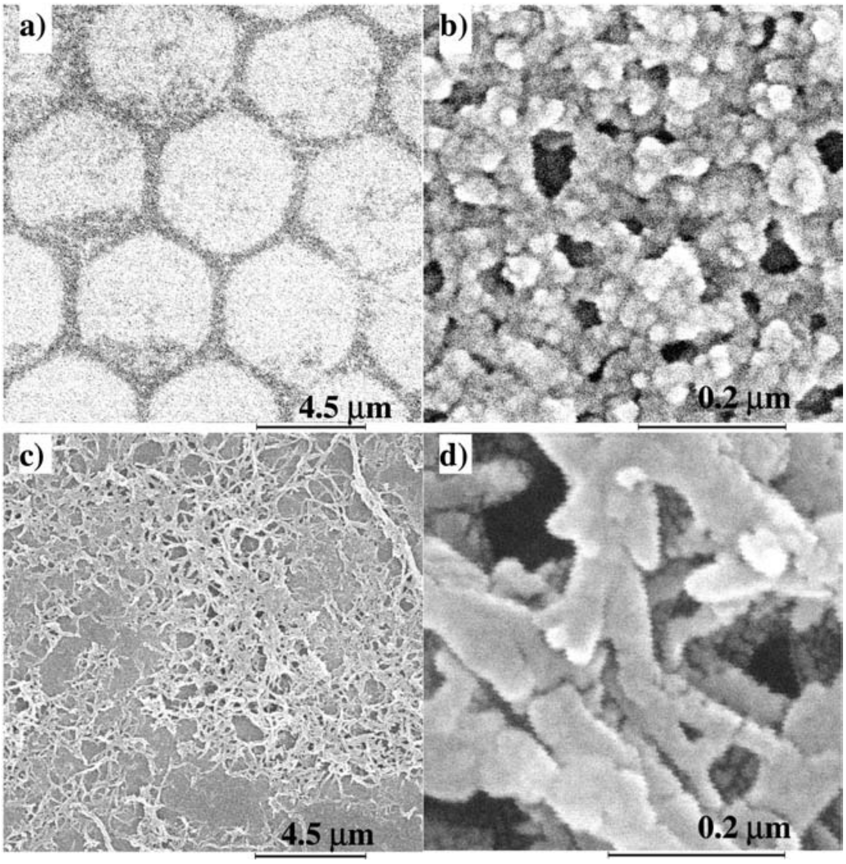

Figure 3. Scanning electron micrographs of poly(aniline) on ITO covered glass with (a and b) and without (c and d) a template. b) and d); higher magnifications

Conclusions

Ordered microporous films were successfully fabricated utilizing amphiphilic block copolymers, poly(acrylic acid)-*block*-poly(styrene) via the controlled condensation and growth of water droplets on the cold surfaces resulting from solvent evaporation of polymer solutions. The higher was the flow rate, the larger became the resulting pores. The copolymer characteristics including the length of hydrophilic and hydrophobic blocks, the concentration of copolymer, and the type of a substrate also have an effect on the pore size and its distribution. It was found that the electropolymerization of aniline in a confined space influences the resulting polymer morphology on the nanometer scale.

References

1. Widawski G, Rawiso M, François B (1994) Nature 369:387
2. François B, Pitois O, François J (1995) Adv Mater 7:1041
3. Jenekhe SA, Chen XL (1999) Science 283:372
4. de Boer B, Stalmach U, Nijland H, Hadziioannou G (2000) Adv Mater 12:581
5. Maeda Y, Koshiyama Y, Shimoi Y, Yonezawa N, Ogino K (2004) Sen'i Gakkaishi 60:268
6. Hayakawa T, Horiuchi S (2003) Angew Chem Int Ed 42:2285
7. Karthaus O, Maruyama N, Cieren X, Shimomura M, Hasegawa H, Hashimoto T (2000) Langmuir 16:6071
8. Nishikawa T, Ookura R, Nishida J, Arai K, Hayashi J, Kurono N, Sawadaishi T, Hara M, Shimomura M (2002) Langmuir 18:5734
9. Srinivasarao M, Collings D, Philips A, Petel S (2001) Science 292:79
10. Peng J, Han Y, Yang Y, Li B (2004) Polymer 45:447
11. Davis KA, Matyjaszewski K (2000) Macromolecules 33:4039
12. Zhang X, Xia J, Matyjaszewski K (2000) Macromolecules 33:2340
13. Ma Q, Wooley KL (2000) J Polym Sci Part A Polym Chem 38:4805
14. Ogino K, Sato H, Tsuchiya K, Suzuki H, Moriguchi S (1995) J Chromatogr A, 699:59
15. Coca S, Davis K, Miller P, Matyjaszewski K (1997) Polym Prepr 38:689
16. Steyer A, Guenoun P, Beysens D, Knobler CM (1990) Phys Rev Lett 42:1086
17. Wang D, Caruso F (2001) Adv Mater 13:350
18. Cassagneau T, Caruso F (2002) Adv Mater 14:34
19. Bartlett PN, Birkin PR, Ghanem MA, Toh CS (2001) J Mater Chem 11:849
20. Guan F, Chen M, Yang W, Wang J, Zhang R, Yang S, Xue Q (2004) Appl Surf Sci 230:131
21. Kim YT, Yang H, Bard AJ (1991) J Electrochem Soc 138:L71
22. Choi SJ, Park SM (2002) J Electrochem Soc 149:E26